Functionalization of Multiwalled Carbon Nanotubes by Atom Transfer Radical Polymerization and Defunctionalization of the Products

Hao Kong, Chao Gao,* and Deyue Yan

College of Chemistry and Chemical Engineering, Shanghai Jiao Tong University, 800 Dongchuan Road, Shanghai 200240, P. R. China

Received February 13, 2004; Revised Manuscript Received April 4, 2004

ABSTRACT: A core−shell hybrid nanostructure, possessing a hard backbone of multiwalled carbon nanotube (MWNT) and a soft shell of brushlike polystyrene (PS), was successfully prepared by in situ atom transfer radical polymerization (ATRP), using Cu(I)Br/*N*,*N*′,*N*″,*N*″-pentmethyldiethylenetriamine (PMDETA) as the catalyst, at 100 °C in diphenyl ether solution. The molecular weight of PS was well controlled, as was the thickness of the shell layer. TEM images of the samples provided direct evidence for the formation of a core−shell structure, i.e., the MWNT coated with polymer layer. FTIR, ^{1}H NMR, SEM, and TGA were used to determine the chemical structure, morphology, and the grafted PS quantities of the resulting products. To further establish the covalent linkage between PS and MWNT moieties, the resulting PS-functionalized MWNTs were defunctionalized by hydrolysis or by thermal decomposition. Comparative studies, based on TEM and SEM images between the PS-functionalized and chemically defunctionalized MWNT samples, also revealed the covalent coating character. GPC analysis showed that the number-average molecular weight (M_n) of the grafted PS chains ranged from 5000 to 11 000 with a relatively broad polydispersity index (PDI, ca. 1.77−3.57). Further copolymerization of *tert*-butyl acrylate (*t*BA) with the PS-linked MWNTs as initiators was realized, illustrating that (1) the PS species is still "living" although the lower controllability of PDI and (2) acrylate-type monomers can be copolymerized with styrene-type ones on the sidewalls of the MWNT. We believe that achieving these hybrid objectives, on the basis of such simple grafting, will pave the way for the design, fabrication, optimization, and eventual application of more functional carbon nanotube-related nanomaterials.

Introduction

Both multiwalled carbon nanotubes (MWNTs) and single-walled carbon nanotubes (SWNTs) possessing tubular nanostructures and unique quantum and promising mechanical properties have been widely considered as attractive candidates for important composition hybrids for fabricating novel materials with desirable properties.[1] Generally, SWNTs exhibit simpler structures and are easily controllable as regards diameter during fabrication as compared with MWNTs. Hence, most previous academic research on carbon nanotubes (CNTs), including functionalization chemistry related to the topic of this paper, is focused on SWNTs. However, as noted by Dalton et al.,[1f] the high cost of SWNTs (ca. \$500 g^{-1} for kilogram-scale production) severely restricts its commercialization for all but very specialized applications. This problem can be mitigated using MWNTs. Fortunately, MWNTs have been scaled up recently by industry, projecting a cost less than \$10 g^{-1}. Most of the excellent properties and merits of MWNTs are comparable with those of SWNTs. Therefore, it is desirable to pay more attention to MWNTs, particularly as regards functionalization, in the future.

Grafting macromolecules onto the convex walls of CNTs, with the aim of improving the processability and extending the applications, has been explored for several years.[2] Remarkable work has been performed in attaching macromolecules to the tips and convex walls of CNTs using the "grafting to" approach via special reactions such as etherification and amidization.[3−7]

More recently, the "grafting from" approach has been employed to functionalize MWNTs and SWNTs,[8] by which method polymer chains can be in situ grafted more densely onto the convex walls of CNTs. Initially, by in situ radical polymerization, polystyrene was grafted onto the MWNT by Shaffer.[8a] Using anionic polymerization, monomers of PS and PVK chains were successfully grafted from the surfaces of SWNTs.[8b,c] However, to control the grafting polymerization, especially the length of the grafted polymer chains, is still attractive. It is well-known that ATRP is one of the most promising polymerization approaches to controlling molecular weight and its distribution within the resulting polymers,[9] by which polymers have been grafted onto the surfaces of nanoparticals, such as silicon, carbon black, Fe_3O_4, etc., to modify surface properties.[10] Via ATRP, some acrylate-type polymers, poly(methyl methacrylate) (PMMA), poly(*n*-butyl methacrylate) (P*n*-BMA), and poly(*tert*-butyl acrylate) (P*t*BA), were grafted onto the SWNTs and MWNTs by three independent groups working simultaneously.[11]

Preliminary work on PMMA-grafted MWNTs in order to obtain different thicknesses of polymer wrapped MWNT has been reported in our previous communication.[11a] However, there are still many questions which cannot easily be answered if only the MMA polymerization system is used. For instance, (1) whether or not this strategy for growth of high density of polymer layers on CNT, especially on MWNTs, can be extended to other ATRP-active vinyl monomers like styrene and acrylamide types; (2) how to control the molecular weight and polydispersity index (PDI) in different monomer systems; and (3) it has been proved that grafted PMMA chains on MWNT are still "living" by further copolymerization of hydroxyethyl methacrylate (HEMA) with the PMMA-coated MWNT as initiators. The question remains regarding other monomer sys-

* Corresponding author: Tel +86-21-5474 2665; Fax +86-21-5474 1297; e-mail chaogao@sjtu.edu.cn.

10.1021/ma049694c CCC: \$27.50
Published on Web 05/07/2004

tems. Obviously, numerous published papers have demonstrated the high controllability for the classic solution or bulk ATRP reaction. Because of the complexity of CNT-supported reactions, ATRP itself, however, one cannot answer in the affirmative the questions before addressing them. For example, three groups reported three different conclusions for CNT-supported ATRP of acrylate-type monomers.[11] Even for the same SWNT system, Adronov et al.[11b] and Ford et al.[11c] obtained conflicting results based on Cu(I)Br/2,2′-bipyridine (bipy) and Cu(I)Cl/bipy catalytic systems, respectively: noncontrollable and well-controllable. Here, we still focus attention on MWNTs for the reason mentioned in the first paragraph. Therefore, this paper aims to (1) extend the monomer system to styrene (PS) for the functionalization of MWNT, (2) investigate the molecular weight and PDI of the coated PS macromolecules by chemical hydrolysis, and (3) copolymerize with styrene- and acrylate-type monomers. In addition, the hydrolyzed and thermally decomposed MWNTs are also characterized in detail so as to further confirm the covalent linkage and decomposition influence on the thermal stability of products.

Experimental Section

Materials. The MWNTs used were purchased from Tsinghua-Nafine Nano-Powder Commercialization Engineering Centre in Beijing. Styrene and *tert*-butyl acrylate (*t*BA) were obtained from Aldrich. The inhibitor was removed by passage through an alumina column and vacuum distillation. CuBr (Aldrich) was purified according to published procedures.[12] 2-Bromo-2-methylpropionyl bromide (α-bromoisobutyryl bromide), ethyl 2-bromoisobutyrate, thionyl chloride ($SOCl_2$), *N*,*N*,*N*′,*N*″,*N*″-pentmethyldiethylenetriamine (PMDETA), and *N*,*N*-(dimethylamino)pyridine (DMAP) were purchased from Acros and used as received. Tetrahydrofuran (THF), *N*,*N*-dimethylformamide (DMF), dimethyl sulfoxide (DMSO), acetone, methanol, ethanol, chloroform ($CHCl_3$), glycol ($HOCH_2$-CH_2OH), diphenyl ether, and other organic reagents or solvents were obtained from Shanghai Reagents Co. They were distilled and kept in the presence of 4 Å molecular sieve to eliminate any traces of water before use. KOH and the 0.22 μm polycarbonate membrane filter were also purchased from Shanghai Reagents Co.

Instrumentation. Molecular weights were measured by gel permeation chromatography (GPC) using PE series 200 with PS as the standard. Fourier transform infrared (FTIR) spectra were recorded on a PE Paragon 1000 spectrometer. Hydrogen nuclear magnetic resonance (^{1}H NMR) spectra were measured with a Varian Mercury Plus 400 MHz spectrometer. Transmission electron microscopy (TEM) analysis was performed on a JEOL JEL2010 electron microscope at 200 kV. Scanning electron microscopy (SEM) images were recorded using a LEO 1550VP field-emission microscope, and the samples were loaded on the glass surface, previously sputter-coated with a homogeneous gold layer for charge dissipation during the SEM imaging. Photographs of samples in solvents were recorded using a digital camera (Sony, DSC-S70). Thermal gravimetric analysis (TGA) was conducted on a PE TGA-7 instrument with a heating rate of 20 °C/min in a nitrogen flow (20 mL/min).

Acid Treatment of MWNTs. A 250 mL flask charged with 5.0 g of crude MWNTs and 100 mL of 60% HNO_3 aqueous solution was sonicated in a bath (40 kHz) for 30 min. The mixture was then stirred for 24 h under reflux. After cooling to room temperature, it was diluted with 200 mL of deionized water and then vacuum-filtered through a 0.22 μm polycarbonate membrane. The solid was washed with deionized water until the pH of the filtrate reached 7. The filtered solid was then dried under vacuum for 12 h at 60 °C to give 3.05 g (~60%) of carboxylic acid-functionalized MWNT (MWNT-COOH).[3]

Scheme 1

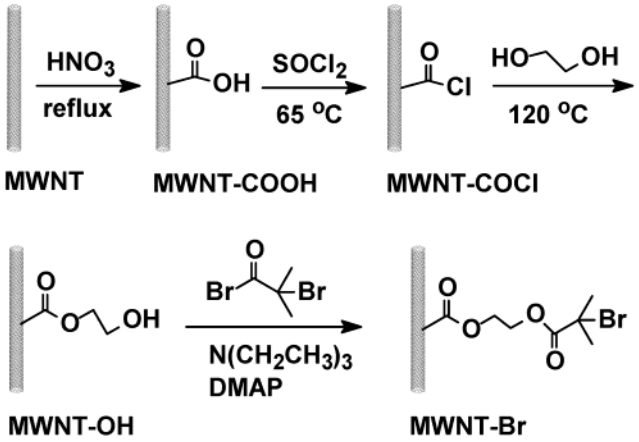

Synthesis of MWNT-OH. Dried MWNT-COOH (0.56 g) was suspended in 20 mL of $SOCl_2$ and stirred at 65 °C for 24 h. The solid was then separated by filtration and washed with anhydrous THF. Subsequently, it was dried under vacuum at room temperature for 2 h to give 0.54 g of carbonyl chloride group-functionalized MWNT (MWNT-COCl). The MWNT-COCl was mixed with 20 mL of glycol and stirred at 120 °C for 48 h. The solid was separated by vacuum filtration using a 0.22 μm polycarbonate membrane as mentioned above and washed with anhydrous THF. After repeated washing and filtration, the resulting solid was dried overnight in a vacuum, to give 0.43 g of hydroxyl group-functionalized MWNT (MWNT-OH).

Synthesis of MWNT-Supported Initiator (MWNT-Br). A 100 mL flask containing MWNT-OH (0.40 g), anhydrous $CHCl_3$ (10.0 mL), DMAP (0.0292 g, 0.2390 mmol), and triethylamine (0.3031 g, 1.667 mmol) was evacuated and thrice filled with Ar. Then 0.3832 g (1.667 mmol) of 2-bromo-2-methylpropionyl bromide dissolved in 5 mL of anhydrous $CHCl_3$ was added dropwise at 0 °C for 60 min. The resulting mixture was stirred for 3 h at 0 °C and then at room temperature for 48 h. The solid was then separated from the mixture by filtration and washed five times with 100 mL of $CHCl_3$. The raw product was dispersed in 20 mL of $CHCl_3$, filtered, and washed three times to remove any adsorbed 2-bromo-2-methylpropionyl bromide. The black solid was collected and dried overnight under vacuum at 40 °C, affording 0.39 g of MWNT-supported ATRP initiator (MWNT-Br). The reaction process is described in Scheme 1. Anal. Found: C, 79.58; H, 2.25; Br, 3.36. This corresponds to ~0.421 mmol initiator groups per gram of MWNT-Br. TGA showed 24.01% weight loss below 450 °C for MWNT-Br and 16.56% weight loss for MWNT-OH. This difference in weight loss corresponds to ~0.448 mmol initiator groups per gram of MWNT-Br.

Synthesis of MWNT-PS. Typically (NTPS1, Table 1), 25.0 mg (0.0105 mmol) of MWNT-Br, 7.2 mg (0.050 mmol) of CuBr, 8.7 mg (0.050 mmol) of PMDETA, and 0.25 mL of diphenyl ether were placed in a 10 mL dry flask, which was then sealed with a rubber plug. The flask was evacuated and filled thrice with Ar. 25.0 mg (0.24 mmol) of styrene was injected into the flask using a syringe. The flask was immersed in an oil bath at 100 °C, and its contents were stirred for 50 h. By the end of the reaction the viscosity had increased dramatically. The mixture was subsequently diluted with $CHCl_3$ and thrice vacuum-filtered using a 0.22 μm polycarbonate membrane. To ensure that no ungrafted polymer or free reagents were mixed in the product, the filtered mass was dispersed in $CHCl_3$, then filtered, and washed with $CHCl_3$. The resulting solid was redispersed in 5 mL of $CHCl_3$ and precipitated by the addition of 100 mL of methanol. The PS-coated MWNT sample (NTPS1) was obtained by filtration and drying overnight under vacuum.

^{1}H NMR ($CDCl_3$) δ (ppm): 7.40−6.30 (−C_6H_5), 4.18 (C*H*Br), 2.25−1.74 [−C*H*(C_6H_5)], 1.74−1.25 [−CH_2−CH(C_6H_5)]. IR (KBr, cm^{-1}): 3020−3080 (aromatic rings), 2960−2822 (−CH_2−).

ATRP of Styrene in the Absence of MWNT. The ATRP polymerization of styrene in the absence of MWNT was carried

Table 1. Polymerization Conditions and Some Results

sample	R_1[a]	R_2[b]	time/h	f_{wt}/%[c]	Y/%[d]	M_n	PDI	T_g/°C grafted	T_g/°C detached
homo-PS		150:1:1[e]	10	100	85	12 800	1.40		98.1
NTPS1	1:1	5:1:1	50	28.6	90	5000	1.77	119	96.5
NTPS2	3:1	15:1:1	50	40.0	70	7900	3.08	113	97.0
NTPS3	5:1	25:1:1	50	48.7	58	8200	3.03	112	97.2
NTPS4	8:1	40:1:1	50	61.5	62	9300	3.20	110	97.5
NTPS5	10:1	50:1:1	50	77.9	65	11 000	3.57	106	97.8

[a] R_1 = monomer:MWNT-Br (wt:wt). [b] R_2 = momoner:CuBr:PMDETA (mol:mol:mol). [c] f_{wt} = the polymer content of the product calculated from TGA data. [d] Yield of product. [e] Monomer:initiator (ethyl 2-bromoisobutyrate) = 150:1 (mol:mol).

out in solution and was used to compare with the synthesis of MWNT-PS. Typically, to a dry flask, 14.3 mg (0.1 mmol) of CuBr, 17.3 mg (0.1 mmol) of PMDETA, 0.9 mL of diphenyl ether, and 1.56 g of styrene (15 mmol) were added, and the flask was sealed with a rubber plug. It was evacuated and thrice filled with Ar gas. After this procedure, 19.5 mg (0.1 mmol) of ethyl 2-bromoisobutyrate was injected into the flask, which was immersed in an oil bath at 100 °C immediately and kept stirring for 50 h. The polymer was isolated by dissolving the mixture in $CHCl_3$, passing it through an alumina column, and then isolated by precipitation with cold methanol. After drying in a vacuum, the homo-PS listed in Table 1 was obtained.

Synthesis of MWNT-PS-*block*-P*t*BA. Further polymerization of *tert*-butyl acrylate (*t*BA) initiated with MWNT-PS (NTPS2) was performed to confirm the "living" character of the MWNT-PS. Typically, 25.3 mg of NTPS2, 5.7 mg (0.040 mmol) of CuBr, 7.0 mg (0.040 mmol) of PMDETA, and 0.25 mL of DMF were placed in a 10 mL flask, which was sealed with a rubber plug. The flask was evacuated and thrice filled with Ar. Following this procedure, 50.6 mg of *t*BA was injected into the flask using a syringe. The flask was then immersed in an oil bath at 60 °C, and its contents were stirred for 48 h. The mixture was then diluted with $CHCl_3$ and vacuum-filtered with a 0.22 μm Millipore polycarbonate membrane. To ensure that no ungrafted polymer or free reagents were mixed with the product, the filtered solid was dispersed in $CHCl_3$, then filtered, and washed. The resulting solid (MWNT-PS-*block*-P*tBA)* was obtained by drying overnight under vacuum.

Defunctionalization of MWNT-PS. A 20 mg sample of as-prepared MWNT-PS was dissolved in 40 mL of THF in a 100 mL round flask fitted with a condenser. Then 10 mL of 1 M KOH/ethanol solution was added to the flask. The contents of the flask were boiled under reflux for 72 h, resulting in the defunctionalized MWNT and detached polystyrene. The solution phase was filtered and evaporated to dryness. The polymer was dissolved in THF and then precipitated by addition of acidified methanol and dried in a vacuum.[12] For the hydrolysis of NTPS5, two samples were prepared. One (CDNT-1) is the solid product washed with alcohol and water to remove KOH. The other (CDNT-2) is the solid product efficiently washed with a large amount of THF and water, which was expected to be free of both PS and KOH.

In addition, the thermally decomposed products made from NTPS3 and NTPS5 (named as TDNT-1 and TDNT-2, respectively) were obtained in situ using the TGA analyzer at 500 °C under a N_2 atmosphere.

Results and Discussion

Preparation of the Precursors. The nanotubes used were MWNTs, which have more walls than SWNTs. The diameters, length, and tips of MWNTs did not vary significantly during the acid-treatment process, although only ca. 60% weight fractions of samples obtained. What we obtained were full length MWNTs with carboxylic acid groups as sidewall, tips, and end defects. It is notable that in some SWNT relevant work the nanotubes were shortened, and the tips were opened in the strong oxidative acid treatment because SWNTs contain only one carbon wall.[2a] From our experience, the walls and CNT lengths and the amount of ropes and masses may be the main factors influencing the solubility and dispersibility of the finally functionalized CNTs.

In recent articles about ATRP processing on the surface of CNTs, the fabrication of CNT-supported initiator is slightly different.[11] In one work, *N*-(4-hydroxyphenyl)glycine and octyl aldehyde were used in the 1,3-dipolar cycloaddition to the sidewalls of SWNTs in order to functionalize them with phenols.[11b] Then the phenols were further functionalized with 2-bromoisobutyryl bromide to generate a SWNT-supported initiator. In another way, 2-hydroxyethyl 2′-bromopropionate and oxidized SWNTs with carboxylic acid groups were prepared individually and then were linked together by etherification.[11c]

Scheme 1 illustrates our synthesis route to the MWNT-supported initiator, named MWNT-Br.[11a] The macroinitiator based on the MWNT was prepared step by step, in which the groups of carboxylic, more reactive carbonyl choloride, hydroxyl, and the initiating sites were linked to the surfaces of MWNTs successively, aiming to simplify the synthesis process, enhance the productivity, and lower the cost of the commercially available cheaper materials.

Even though the raw carbon nanotubes and the synthesis processes of macroinitiators are different from each other, polymer layers were all successfully grown onto the surfaces of SWNT or MWNT via the ATRP approach, but with distinct polymerization control.

In our experiments, the filtration and washing process were essential and important in every fabricating step. The small molecules absorbed on the MWNTs must be removed by carefully washing to guarantee that the MWNT-based macroiniators are as pure as possible.

As an important argument, the TGA analysis of the intermediates indicates that carboxylic acid groups, hydroxyl groups, and initiating sites had been covalently linked to the MWNT sidewalls. The MWNTs show good thermal stability below 650 °C. When MWNTs was functionalized as MWNT-COOH, there was a continuous but not very obvious decrease in weight. The onset temperatures for MWNT-OH and MWNT-Br are ~310 and 277 °C (very similar to those of products made from other separated batchs[11a]), respectively, while the boiling points (bp) of glycol and 2-bromo-2-methylpropionyl bromide are only 196 and 162 °C, respectively. The mixed sample of crude MWNT and glycol or 2-bromo-2-methylpropionyl bromide exhibited an onset temperature below 200 °C. The data indicated that glycol and 2-bromo-2-methylpropionyl bromide had been covalently linked to MWNT in the MWNT-OH and MWNT-Br.

FTIR spectra contained the peak signal for carbonyl bonds (C═O) in the precursors. In FTIR measurements, the amount of sample added to the KBr disk must be strictly controlled so that it is less than the amount

Scheme 2

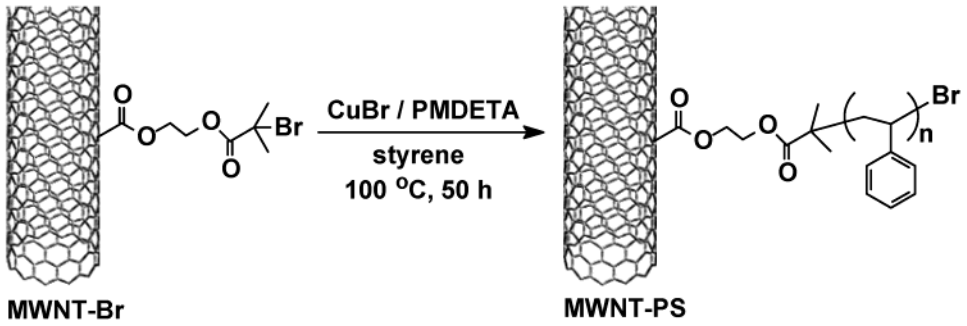

required for normal FTIR detection because the black MWNT would absorb all the infrared rays if the amount of MWNT were too much. Therefore, only a very weak C═O stretch (ca. 1730 cm^{-1}) beside the strong aromatic C═C stretch (ca. 1634 cm^{-1}) can be found for the MWNT-COOH. For MWNT-OH or MWNT-Br, the stronger C═O absorption peaks were observed (see Figure 1). Judging by combination of TGA and FTIR results, we can say that the initiating sites of ATRP have been covalently anchored to the MWNT.

More effective approaches, which would give strong signals due to the covalent bonds between small molecules and the convex surface of MWNTs, have not been found in our characterization. Raman analysis of our samples was also tried, but no considerable signals were observed in the spectra. The ^1H NMR peaks were not detected, which may be attributed to the fact that the chain of small molecules attached on the MWNT is too short to detect.

Preparation of MWNT-PS. As far as we know, styrene is among the alkenes first used in the ATRP.[9] The molecular weight and PDI can be well controlled, either in bulk or in solution, based on the Cu(I)/Cu(II) redox process. For the macroinitiator, MWNT-Br, the solvent is necessary, especially in the reactions with lower monomer:MWNT-Br feed ratios. Thus, diphenyl ether was chosen as the solvent in our experiments to dilute the monomer and wet the initiators.

The synthesis of MWNT-PS is displayed in Scheme 2. After 50 h of polymerization at 100 °C, the reaction system became thick or solidified, suggesting that the polymerization had taken place. After the filtrating, washing, and drying of the product, a gray powder was obtained. The products turned from dark gray to off-white with increasing polymer content. The reaction conditions and results are summarized in Table 1.

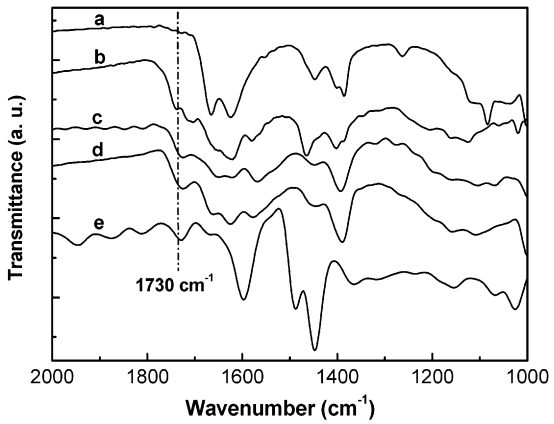

Figure 1. FTIR spectra of crude MWNT (a), MWNT-COOH (b), MWNT-OH (c), MWNT-Br (d), and NTPS5 (e).

It was found that the number-average molecular weight (M_n) of the grafted PS chains, obtained by hydrolysis of MWNT-PS, increased regularly with increasing styrene:MWNT-Br weight feed ratio (R_1), which indicated that the molecular weight of the grafted PS on the surfaces of MWNT can be relatively controlled by the ATRP approach. On the other hand, the PDI of the grafted PS is considerably broader than that (1.40) of the homo-PS, generated by the conventional ATRP of styrene initiated with ethyl 2-bromoisobutyrate without MWNT-Br, particularly for the samples with a higher feed ratio. The broader PDI was likely to arise from the heterogeneous surface initiating, confined propagating, or couple termination of part-polymer chains. In the reaction mixture, some of the macroinitiators (e.g., individual tubes) are more soluble, some are more dispersible (e.g., bundles and ropes), and others are less dispersible (e.g., the jointed masses). Even on the same tube, the densities or concentrations of local initiating points are different from each other because of different defect dispersion and different degree of oxidation. These factors would result in gradient initiating rates and then broader PDI. On the MWNT surfaces, the space among tubes is different because of the existence of bundles, ropes, and masses. On the surfaces with very limited space, the polymer would cease propagating when it approached other confining surfaces. This confined degree strongly depends on the local tubes. So polymer chains stop their "growing" at different times and with different lengths, resulting in broader PDI. Besides, because the local concentration of initiating points in some surface segments is so high, the propagating polymer chains can be terminated by coupling with each other, which would also lead to broader PDI. Because of such reasons, different carbon nanotubes and different acid treatment processes would lead to discrepancies and distinct conclusions. Obviously, either confined propagating or couple termination will make the further copolymerization impossible. The fact of successful copolymerization (discussed below) excludes the strong effects of the two factors. Thus, we believe that the main reason for broader PDI in MWNT-supported polymerization is gradient initiating and propagating rates. On the other hand, PDI of homopolymers made by ATRP in homogeneous solution is also relatively broader, typically 1.2−1.7. In our experiments, PDI of homo-PS is ~1.35−1.51. However, such broad PDI almost has no influence on the further copolymerization with the homopolymer as initiators. Therefore, the reasons for broader PDI of polymers in MWNT systems are very complex, but copolymerization can still be performed with MWNT-PS as initiators.

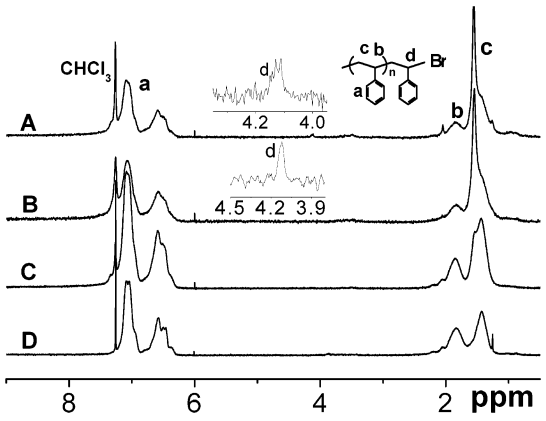

Figure 2. ^{1}H NMR ($CDCl_3$) spectra of NTPS1 (A), NTPS3 (B), NTPS5 (C), and detached PS (D).

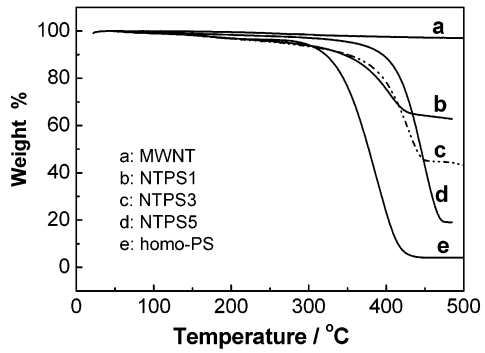

Figure 3. TGA curves of crude MWNT and some samples of MWNT-PS.

Figure 1e shows a FTIR spectrum of NTPS5, in which the absorption bands assigned to C−H stretch (ca. 3025 cm^{-1}) from the aromatic rings, C−H stretch (ca. 2900 cm^{-1}) from the alkyl portions, and C═C stretch (ca. 1634 cm^{-1}) are clearly observed. Other samples of PS-coated MWNTs showed almost the same spectra as NTPS5.

The chemical structure of the samples of MWNT-PS was further characterized by ^{1}H NMR (Figure 2). The inherent peaks of PS macromolecules such as those of benzene rings, methylene (−CH_2−), and tertiary carbon hydrogen [−C*H*(C_6H_5)−] clearly appear in the spectra at 7.40−6.30, 1.74−1.25, and 2.25−1.74 ppm, respectively. Significantly, when the M_n of the grafted PS chains are lower (from NTPS1 to NTPS3), the hydrogen atom of terminal units (C*H*Br) is found in the ^{1}H NMR spectrum as a peak at ∼4.18 ppm, which provides strong evidence for the "living" feature of the complex polymerization. So it is expected to initiate other monomers with MWNT-PS as initiators, to grow block copolymers on the surfaces of MWNT. The relevant experiments have been carried out and will be discussed in the section "copolymerization". When the M_n of the PS chains becomes higher (for NTPS5), the unique signal becomes too weak to detect.

Figure 3 displays the TGA curves of some samples of MWNT-PS and homo-PS. The content of the polymer shell calculated from the TGA data ranges from 28.6% to 77.9% (Table 1). The onset of the decomposition temperature (T_d) of the PS moieties in MWNT-PS approached 380−410 °C, 50−80 °C higher than that (ca. 330 °C) of homo-PS although the homo-PS has a higher M_n (12 800) and a narrower PDI (1.40). The T_d of the grafted PS moieties also rises with increasing M_n. Therefore, the thermal stability of the PS chains can be dramatically improved by linkage with MWNT.

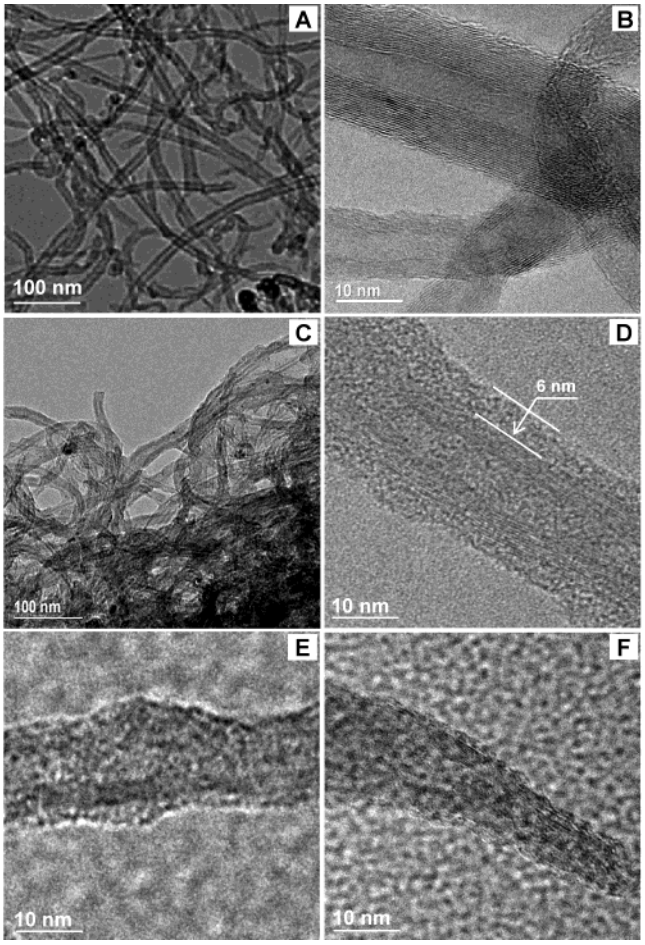

Figure 4. TEM images of crude MWNT (A, B), NTPS5 (C, D), NTPS3 (E), and NTPS1 (F).

DSC measurements show that the glass transition temperature (T_g) of the grafted PS chains is greater than that of the corresponding detached PS sample, by about 10−20 °C (Table 1). Similar phenomena were also observed in PMMA grafted SWNT systems.[11b] Interestingly, T_g of the grafted PS chains decreases with increasing M_n, which is contrary when compared with the general rule for T_g of detached polymers. It could be explained that the confining of one end of the polymer chain on the MWNT would restrict the movement and vibration of the whole chain and so have an effect on the T_g, and the longer the chain was, the less the effect on the T_g would be.

All of the aforementioned data effectively demonstrate the in situ ATRP reaction on the MWNT surfaces has been successful, and PS chains with various molecular weights have been covalently anchored to MWNT. However, some questions still exist: (1) Where are the polymer chains rooted: only at the tips or on the full convex surfaces? (2) Can the linked macromolecules separate the MWNT ropes and the masses welded together into individual tubes? (3) The thickness of the polymer layers on various tubes and on the same tube is uniform or not if the polymer chains enwrap MWNT, forming the so-called core−shell structure? Further measurements of TEM and SEM would give the answers.

The TEM images of the crude and functionalized MWNTs are shown in Figure 4. The average internal and external diameters of the crude nanotubes are about 5−10 and 20−30 nm, respectively. The MWNT wall

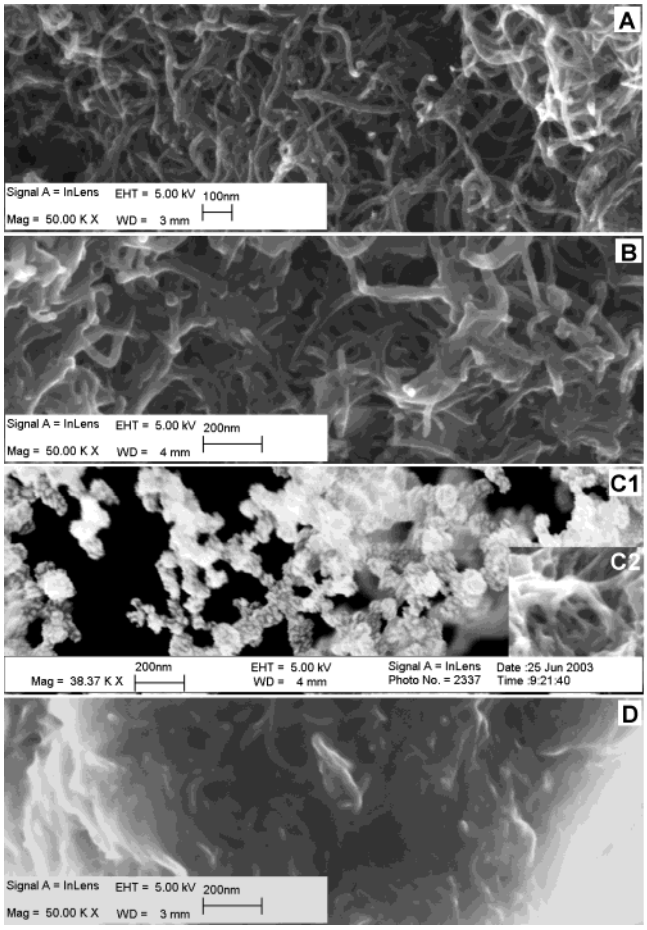

Figure 5. SEM images of crude MWNT (A), NTPS1 (B), NTPS3 (C1, C2), and NTPS5 (D).

consists of 10−25 graphite layers. The average length of the MWNT is approximately several micrometers. In the images of crude MWNTs (Figure 4A), individual tubes separated from each other are obviously found, and no extra phase marked with different degrees of gray can be detected in the high-resolution image (Figure 4B). For the samples of MWNT-PS, in the lower amplification image (Figure 4C), it can be found that some parts of the tubes are clothed with a polymer layer, and the jointed tubes still mass together. This indicates that (1) the thickness of the polymer layer coated on the MWNT is not completely same, (2) the initiating and propagating of polymerization occur not only at the tips but also on the whole convex surfaces, and (3) the grown macromolecular chains cannot disperse the massed tubes, at least not so fully. In the high-resolution images (e.g., Figure 4D), the core−shell structure is very clear. The carbon tube has been constructed from graphite lamella layer-by-layer, and the polymer shell is vividly impinged on the outer wall along the tube stretched direction. It can be also found that the thickness of polymer shell imaged on the right side is slightly higher than that on the left side. In the center, along the tubular hollow, the polymer image also can be easily recognized if compared with the image of crude MWNT. In addition, the average thickness of the shell decreases with decreasing M_n and polymer content (Figure 4E,F). As a comparison, no polymer shell outside nanotubes was observed under the TEM for the samples of mixtures of MWNT and PS.

Figure 5 displays the SEM images of crude MWNTs and samples of MWNT-PS. The MWNTs were clearly observed lying on the gold layer in the image with a 50 000 magnification (Figure 5A). The convex surfaces of crude MWNTs seem to be smooth with nothing adhering to them. In contrast, in the three SEM images of MWNT-PSs with different polymer content, the samples distinguish themselves from each other by various appearances, which change with the changing of R_1. In detail, NTPS1, with the lowest polymer content, seems to be still nanotube-like, only the diameters increasing by several nanometers (Figure 5B). This MWNT pattern resembles logs. In some images of NTPS3 (Figure 5C1), interesting patterns, looking like snow-covered trees, are observed. This could be caused by interactions among the PS chains and the PS-functionalized MWNTs. This investigation is in progress and will be reported on later. In other images of NTPS3, general polymer-coated MWNT patterns are also found (inserted C2). When the polymer content was increased, e.g., NTPS5, the polymer formed a continuous phase, and the MWNTs were submerged in the polymer phase, just like roots embedded in the soil (Figure 5D). The SEM images also show the evenly covalent grafting feature, and the coated shell thickness increases with the increasing amount of polymer.

The solubility or dispersibility of the samples is illustrated in the section "solubility of the samples".

Chemical Hydrolysis of MWNT-PS. To recover the MWNTs from the PS grafted products and then characterize them is another highlight that we concerned with. We hoped to find out some useful information resulting from the defunctionalization process to further confirm covalent linkage and to initially explore the thermal decomposition mechanism of the functionalized MWNT that was rarely reported up to now.

The first approach used was base hydrolysis of esters, which act as bridges between the PS chains and the MWNT surfaces of MWNT-PS samples. Theoretically, three products—MWNT-COOH, glycol, and PS—could be obtained as a result of complete hydrolysis of the ester bonds. However, only MWNT solids and polymers were collected in our experiments. The detached PS was used to measure its molecular parameter such as M_n and PDI and thermal properties such as T_g. The residual MWNT samples were mainly characterized by TEM, SEM, and TGA.

The peeled NTPS5 samples, as one typical example, obtained from the basic hydrolysis, are named CDNT-1 and CDNT-2. CDNT-1 was filtered, and this solid collected by restricted washing with alcohol and water. CDNT-2 was the solid washed efficiently with THF and water. TGA analysis showed the presence of CDNT-1 still mixed with ∼25% polymer. No polymer weight loss was detected in the TGA curve of CDNT-2.

It is interesting that some PS nanoparticles were found in both SEM and TEM images of CDNT-1 (some polymer phases were marked by arrows, see Figure 6A−C) and not found in those of CDNT-2 (Figure 6D) and MWNT-PSs, in accordance with the prediction. The phase separation occurred between the detached PS and the residual MWNTs in water and alcohol, forming the PS nanoparticles. The mixed PS can be removed by washing with a large amount of THF, which verified again that the PS chains in MWNT-PS were covalently linked to the convex MWNT surface for the samples of MWNT-PS. Otherwise, the free polymer chains would have been removed by repeated washing with good solvents followed by filtering, and the separated phases

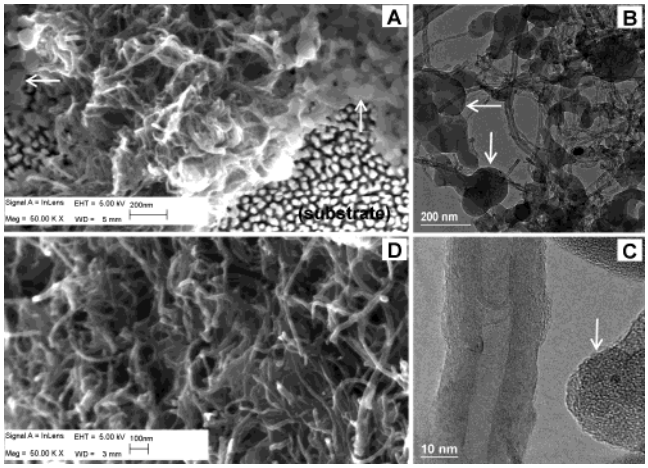

Figure 6. SEM image of CDNT-1 (A), TEM images of CDNT-1 (B, C), and SEM image of CDNT-2 (D).

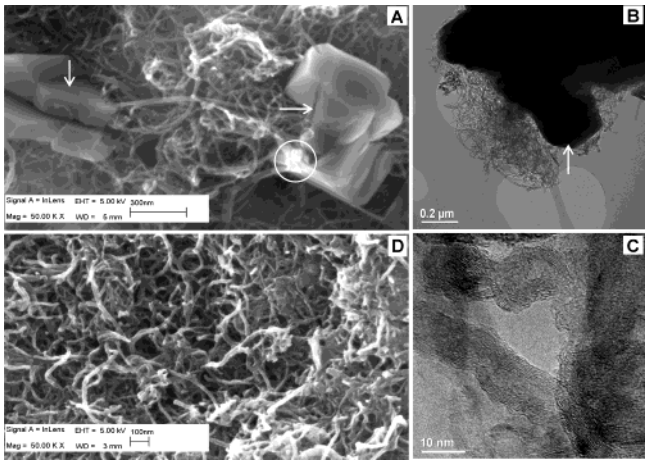

Figure 7. SEM image of TDNT-2 (A), TEM images of TDNT-2 (B, C), and SEM image of TDNT-1 (D).

would be observed for MWNT-PS if considerable amounts of PS were mixed in the system.

Thermal Decomposition of MWNT-PS. Another technique we used to defunctionalize MWNT-PS involved complete thermal decomposition of the polymer shell, resulting in uncovered MWNTs without carboxylic acid groups. The PS shell is virtually decomposed, fully approaching 500 °C according to the TGA analysis of samples. Therefore, 500 °C was chosen as the terminal temperature in the defunctionalization experiments.

The residual compounds obtained after thermal decomposing NTPS3 and NTPS5 were denoted as TDNT-1 and TDNT-2, respectively. In the SEM images, part of TDNT-2 also maintains the morphology of MWNT. However, it is notable that part of TDNT-2 has been converted into amorphous carbon (Figure 7A). In the TEM image of TDNT-2, amorphous carbon masses are also observed (Figure 7B). In the high-resolution image (Figure 7C), it is found that the original tubes have been twisted and distorted after the thermal decomposition. TDNT-1 still looks like MWNT, and significant destruction is rarely observed (Figure 7D). These images suggested that the covalently functionalized moieties on the MWNT have strong negative influence on the thermal degradation of carbon nanotubes, and the more the functionalized moieties are, the stronger the influence is. The kinetics and mechanism of the thermal degradation are under investigation.

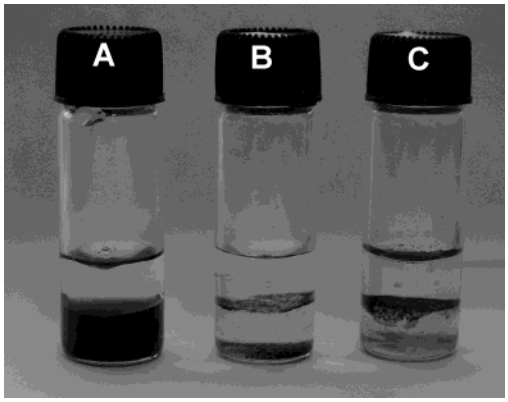

Figure 8. Photo of NTPS3 (A), TDNT-1 (B), and CDNT-2 (C) placed in $CHCl_3/H_2O$ mixture solvents.

Solubility of the Samples. Because the MWNT ropes and masses cannot be totally separated into individual tubes by functionalization, most of the functionalized tubes still have a length of at least several or even tens of micrometers, so the solubility or dispersibility of functionalized MWNT is generally lower than that of comparably functionalized SWNT.

The obvious variation in solubility or dispersibility for functionalized MWNT samples during the synthesis process still indicated the covalent linkage between various functional groups and MWNT. The crude MWNT cannot dissolve in any solvents we tested. After treating MWNT with HNO_3, the resulting MWNT-COOH can be poorly dispersed in water and aggregated on the interface of chloroform and water. MWNT-OH shows better dispersibility than MWNT-COOH in water and organic solvents. MWNT-Br exhibited very poor dispersibility in water but relatively good solubility in organic solvents. When the PS chains were attached to the walls of the nanotubes, the MWNT-PS showed a relatively good solubility in some solvents such as THF, $CHCl_3$, and toluene, almost similar to that of pure PS. During hydrolysis some black solid deposited from the reaction mixture and aggregated on the bottom of reaction vessel. After repeated washing, this solid showed poor solubility in the solvents used, just as the MWNT-COOH did. The solubility for the samples generated by thermal defunctionalization was markedly similar to the crude MWNTs. The evolution of the solubility of the MWNT-contained samples verified that every step of the modification was successful, and the carboxyl groups, hydroxyls, the initiating moieties sites of ATRP, and the PS chains did covalently link to the convex walls of MWNT.

Figure 8 gives the digital photos of the samples of NTPS3, TDNT-1, and CDNT-2 placed in the incompatible solvent system ($H_2O/CHCl_3$). The MWNT-PS is soluble in $CHCl_3$ and insoluble in H_2O. The clear interface between H_2O and $CHCl_3$ solution can be observed after adding MWNT-PS to the $H_2O/CHCl_3$ system. After the thermal and chemical defunctionalization, the resulting nanotubes TDNT-1 and CDNT-2 did not dissolve in both $CHCl_3$ and H_2O. However, more CDNT-2 solids formed by chemical hydrolysis aggregate onto the interface between water and chloroform than TDNT-1 produced by the thermal decomposition. This can be attributed to the facts that the hydrophilic carboxyl groups are retained after chemical hydrolysis, while the thermal defunctionalization at 500 °C almost completely decomposes the carboxyl and other attached groups.

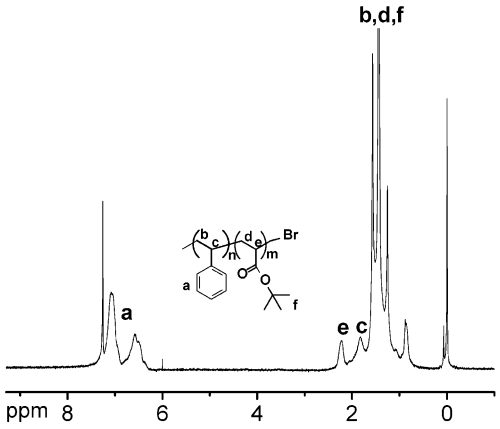

Figure 9. ^{1}H NMR spectrum of MWNT-PS-*block*-P*t*BA in $CDCl_3$.

The polymer content of MWNT-PSs samples influences the solubility in organic solvents. NTPS1, with 28.6% polymer fraction, showed good solubility in $CHCl_3$, forming a black solution which is stable for several weeks. But NTPS5, containing 77.9% polymer, is only stable in $CHCl_3$ for several hours, and the black product floats and assembles on the upper layer of solvent to form a black layer. NTPS3, like NTPS5, would float to the surface of solvent, too, but it be stable in the solvent for several days. In other solvents of somewhat lower density, such as THF, toluene, etc., this phenomenon could be observed, too, but is not so obvious. This may be due to the lower density of MWNT-PS after functionalization or by cross-linking between functionalized MWNT, as pointed out by Adronov et al.[11b] in their polymer-coated SWNT system. Here, we believe that the lower density plays the main role because many separated tubes are also observed in the TEM images although the local cross-linking factor cannot be excluded totally. In fact, for the MWNT, there are many jointed masses in the acid-treated samples, as mentioned above. It is impossible to tear up such masses just dependent on polymerization. Therefore, the polymer-coated tubular masses and many of the ropes would float in the solvents of higher density. Such floating phenomena suggests that (1) the MWNTs are covalently linked with polymer grafts, (2) such linkage strongly influences the physical properties of the tubes, and (3) the so-called solution of functionalized MWNT is not a "true solution" as compared with the classic solution of small molecules because of their giant molecular weights ($>10^{10}$) per one functionalized tube. It is unimaginable if the joint masses could be formed into a true solution despite soluble polymers are coated on their surfaces. On the other hand, although such functionalized MWNTs cannot be truly soluble, their dispersibility and processability can be dramatically improved, and their properties can also be changed and tailored. Hence, we believe the significance of functionalization research of MWNTs will not be weakened due to the solubility.

Copolymerization. To confirm the "living" character of as-prepared MWNT-PS, further copolymerization of *t*BA initiated with NTPS2 was performed, resulting in MWNT-PS-*b*-P*t*BA. Again, the length of P*t*BA blocks increased if the feed ratio (*t*BA:NTPS2) rose. The resulting products were fully characterized by TGA, ^{1}H NMR, SEM, TEM, and FTIR, definitely proving the success of block copolymerization. Figure 9 gives the ^{1}H NMR spectrum of one copolymer-functionalized MWNTs. The P*t*BA:PS unit ratio calculated from this spectrum is ~0.75/1.

Further hydrolysis of the *tert*-butyl groups of P*t*BA blocks in the presence of CF_3COOH gave rise to poly(acrylic acid)-*block*-polystyrene functionalized MWNT, a novel amphiphilic core−shell nanoobject. The details on the copolymerization and hydrolysis will be published elsewhere. The realization of copolymerization on the surfaces of MWNTs would dramatically expand the functionalization chemistry and material fields of carbon nanotubes.

Conclusions

The functionalization of MWNTs with PS via in situ ATRP and the chemical and thermal defunctionalizations of the functionalized MWNT were wholly investigated in this work. After the initiating sites were introduced onto the convex walls of MWNT, the ATRP initiated by the MWNT with initiating sites in the presence of Cu(I)Br/PMDETA was successfully performed, and the polymerization was confined to the surface of MWNT, forming the core−shell nanostructure (i.e., the MWNT coated by a PS shell). However, the PDI of the PS chains was broader than that of the PS samples generated in the conventional ATRP, even though the molecular weight of the grafted PS chains was well controlled. The PS-functionalized MWNT was confirmed by TGA, FTIR, ^{1}H NMR, TEM, and SEM. Furthermore, the defunctionalization of the functionalized MWNT was realized through chemical hydrolysis or thermal decomposition. The phase separation between detached PS and MWNT was clearly observed for the sample made by inefficient washing, and the PS phase can be fully removed from the hydrolyzed mixture by washing with suitable solvents. Such phase separation behavior provides counterevidence to prove the covalent grafting in the polymer-functionalized samples. The decomposition of polymer moieties has a bad influence on the thermal stability of nanostructures of residual MWNT.

Despite the broader PDI of the grafted PS chains, they are still "living". Depending on the terminal initiating sites, poly(*tert*-butyl acrylate) was blocked with PS, giving PS-*block*-PtBA-coated MWNT. The mechanical, electrical, and other related properties of the resulting nanoobjects are also interesting for us and will be accordingly addressed soon. We believe that this methodology can be used in the synthesis of other polymer-coated carbon nanotubes with increasing complexity and functionality in the polymeric shells. The realization of polymerization and block copolymerization of both acrylate- and styrene-type monomers on MWNT by the convenient ATRP grafting from strategy would pave the way for the fabrication and application of more CNT−polymer composites and nanomaterials.

Acknowledgment. We acknowledge funding support from the National Natural Science Foundation of China (No. 20304007), Rising-Star Foundation of Shanghai (No. 03QB14028), and the Opening Research Foundation of the Key Laboratory of Molecular Engineering of Polymers of Fudan University. We thank Mr. Songhai Xie (TEM), Ms. Ying Chen (TEM), Ms. Ruibin Wang, and Ms. Pinfang Zhu (SEM) for their technical assistance and Prof. David R. M. Walton and Mr. Yizheng Jin for helpful discussions.

References and Notes

(1) (a) Iijima, S. *Nature (London)* **1991**, *354*, 56. (b) Dai, L.; Mau, A. W. H. *Adv. Mater.* **2001**, *13*, 899. (c) Wang, X.; Liu, Y.; Zhu, D. *Adv. Mater.* **2002**, *14*, 165. (d) Banerjee, S.; Kahn, M. G. C.; Wong, S. S. *Chem.—Eur. J.* **2003**, *9*, 1898. (e) Niyogi, S.; Hamon, M. A.; Hu, H.; Zhao, B.; Bhowmik, P.; Sen, R.; Itkis, M. E.; Haddon, R. C. *Acc. Chem. Res.* **2002**, *35*, 1105. (f) Dalton, A. B.; Collins, S.; Razal, J.; Munoz, E.; Ebron, V. H.; Kim, B. G.; Coleman, J. N.; Ferraris, J. P.; Baughm, R. H. *J. Mater. Chem.* **2004**, *14*, 1.

(2) (a) Liu, J.; Rinzler, A. G.; Dai, H.; Hafner, J. H.; Bradley, R. K.; Boul, P. J.; Lu, A.; Terry, I.; Konstantin, S.; Huffman, C. B.; Rodriguez-Macias, F.; Shon, Y.-S.; Lee, T. R.; Colbert, D. T.; Smalley, R. E. *Science* **1998**, *280*, 1253. (b) Chen, J.; Hamon, M. A.; Hu, H.; Chen, Y.; Rao, A. M.; Eklund, P. C.; Haddon, R. C. *Science* **1998**, *282*, 95. (c) Kovtyukhova, N. I.; Mallouk, T. E.; Pan, L.; Dickey, E. C. *J. Am. Chem. Soc.* **2003**, *125*, 9761.

(3) (a) Riggs, J. E.; Guo, Z.; Carroll, D. L.; Sun, Y.-P. *J. Am. Chem. Soc.* **2000**, *122*, 5879. (b) Huang, W.; Taylor, S.; Fu, K.; Lin, Y.; Zhang, D.; Hanks, T. W.; Rao, A. M.; Sun, Y.-P. *Nano Lett.* **2002**, *2*, 311. (c) Sun, Y.-P.; Fu, K.; Lin, Y.; Huang, W. *Acc. Chem. Res.* **2002**, *35*, 1096. (d) Fu, K.; Huang, W.; Lin, Y.; Riddle, L. A.; Carroll, D. L.; Sun, Y.-P. *Nano Lett.* **2001**, *1*, 439.

(4) (a) Shaffer, M. S. P.; Windle, A. H. *Adv. Mater.* **1999**, *11*, 937. (b) Chen, R. J.; Zhang, Y.; Wang, D.; Dai, H. *J. Am. Chem. Soc.* **2001**, *123*, 3838. (c) Shim, M.; Javey, A.; Kam, N. W. S.; Dai, H. *J. Am. Chem. Soc.* **2001**, *123*, 11512.

(5) (a) Sano, M.; Kamino, A.; Okamura, J.; Shinkai, S. *Langmuir* **2001**, *17*, 5125. (b) Pantarotto, D.; Partidos, C. D.; Graff, R.; Hoebeke, J.; Briand, J.-P.; Prato, M.; Bianco, A. *J. Am. Chem. Soc.* **2003**, *125*, 6160. (c) Saini, R. K.; Chiang, I. W.; Peng, H.; Smalley, R. E.; Billups, W. E.; Hauge, R. H.; Margrave, J. L. *J. Am. Chem. Soc.* **2003**, *125*, 3617.

(6) (a) Frehill, F.; Vos, J. G.; Benrezzak, S.; Koos, A. A.; Konya, Z.; Ruther, M. G.; Blau, W. J.; Fonseca, A.; Nagy, J. B.; Biro, L. P.; Minett, A. I.; in het Panhuis, M. *J. Am. Chem. Soc.* **2002**, *124*, 13694. (b) Banerjee, S.; Wong, S. S. *J. Am. Chem. Soc.* **2002**, *124*, 8940. (c) Ravindran, S.; Chaudhary, S.; Colburn, B.; Ozkan, M.; Ozkan, C. S. *Nano Lett.* **2003**, *3*, 447.

(7) (a) Gao, M.; Huang, S.; Dai, L.; Wallace, G.; Gao, R.; Wang, Z. *Angew. Chem., Int. Ed.* **2000**, *39*, 3664. (b) Kang, Y.; Taton, T. A. *J. Am. Chem. Soc.* **2003**, *125*, 5650. (c) Kim, O.-K.; Je, J.; Baldwin, J. W.; Kooi, S.; Pehrsson, P. E.; Buckley, L. J. *J. Am. Chem. Soc.* **2003**, *125*, 4426. (d) Zhao, W.; Song, C.; Pehrsson, P. E. *J. Am. Chem. Soc.* **2002**, *124*, 12418.

(8) (a) Shaffer, M. S. P.; Koziol, K. *Chem. Commun.* **2002**, 2074. (b) Viswanathan, G.; Chakrapan, N.; Yang, H.; Wei, B.; Chung, H.; Cho, K.; Ryu, C. Y.; Ajayan, P. M. *J. Am. Chem. Soc.* **2003**, *125*, 9258. (c) Wu, W.; Zhang, S.; Li, Y.; Li, J.; Liu, L.; Qin, Y.; Guo, Z.-X.; Dai, L.; Ye, C.; Zhu, D. *Macromolecules* **2003**, *36*, 6286.

(9) (a) Wang, J. S.; Matyjaszewski, K. *J. Am. Chem. Soc.* **1995**, *117*, 5614. (b) Coessens, V.; Pintauer, T.; Matyjaszewski, K. *Prog. Polym. Sci.* **2001**, *26*, 337. (c) Qiu, J.; Charleux, B.; Matyjaszewski, K. *Prog. Polym. Sci.* **2001**, *26*, 2083. (d) Matyjaszewski, K.; Xia, J. *Chem. Rev.* **2001**, *101*, 2921.

(10) (a) Liu, T.; Jia, S.; Kowalewski, T.; Matyjaszewski, K.; Casado-Portilla, R.; Belmont, J. *Langmuir* **2003**, *19*, 6342. (b) Mandal, T. K.; Fleming, M. S.; Wait, D. R. *Nano Lett.* **2002**, *2*, 3. (c) Wang, Y.; Teng, X.; Wang, J.-S.; Yang, H. *Nano Lett.* **2003**, *3*, 789. (d) Carrot, G.; Diamanti, S.; Manuszak, M.; Charleux, B.; Vairon, J.-P. *J. Polym. Sci., Part A: Polym. Chem.* **2001**, *39*, 4294.

(11) (a) Kong, H.; Gao, C.; Yan, D. *J. Am. Chem. Soc.* **2004**, *126*, 412. (b) Yao, Z.; Braidy, N.; Botton, G. A.; Adronov, A. *J. Am. Chem. Soc.* **2003**, *125*, 16015. (c) Qin, S.; Qin, D.; Ford, W. T.; Resasco, D. E.; Herrera, J. E. *J. Am. Chem. Soc.* **2004**, *126*, 170.

(12) Cheng, G.; Böker, A.; Zhang, M.; Krausch, G.; Müller, A. H. E. *Macromolecules* **2001**, *34*, 6883.

MA049694C